

# Thermodynamic Properties of Solid Ar, Kr, and Xe Based Upon a Short-Range Central Force and the Conventional Perturbation Expansion of the Partition Function

M. L. KLEIN

*Division of Pure Chemistry, National Research Council of Canada, Ottawa, Ontario, Canada*

AND

G. K. HORTON

*Physics Department, Rutgers University, New Brunswick, New Jersey 08903*

AND

J. L. FELDMAN\*

*Physics and Astronomy Department, Rensselaer Polytechnic Institute, Troy, New York 12181*

(Received 13 January 1969)

Thermodynamic properties of the rare-gas solids Ar, Kr, and Xe are calculated using phenomenological two-body central potentials. The cubic and quartic anharmonic terms in the crystal Hamiltonian have been included, using conventional perturbation theory. Although some definite discrepancies with experiment exist for  $T < \frac{1}{3}T_{\text{melting}}$ , these simple models give a fair over-all account of both the volume and temperature dependence of the Helmholtz energy. However, for  $T > \frac{1}{3}T_{\text{melting}}$  (rms deviations greater than  $\sim 6\%$  of the nearest-neighbor distance), anharmonic contributions to the thermodynamic properties become unrealistically large, indicating, we believe, the breakdown of perturbation theory to the order considered in this work.

## 1. INTRODUCTION

SOME years ago, quasiharmonic theories<sup>1</sup> of solid Ar were stimulated by a new and precise measurement<sup>2</sup> of the heat capacity. The comparison of theory with experiments leads to some rather disappointing results. Quite apart from the problem of the uncertainty in the interatomic potential, assumed to take the familiar Lennard-Jones form, the magnitude of the zero-temperature Debye theta  $\Theta_0^\circ$  and the high-temperature behavior of  $\Theta^\circ(T)$  could not be properly understood, and it was conjectured that anharmonic effects were responsible.

At the same time a quantum version of the perturbation theory of anharmonic phonon interactions, known since the work of Born and Brody, was presented<sup>3</sup> and further developed, especially by Maradudin and collaborators.<sup>4</sup> In particular, the latter authors showed that

explicit numerical calculations were feasible. The first realistic anharmonic calculation for the inert-gas solids was that of Barron and Klein<sup>5</sup> who studied the anharmonic contribution to  $\Theta_0^\circ$ . More recently, Simmons and his co-workers<sup>6</sup> have produced a wealth of new and precise experimental data on the lattice constant and its pressure dependence. To this was added more modern specific-heat data by Finegold and Philips,<sup>7</sup> Serin and collaborators.<sup>8,9</sup> The present time, therefore, seems opportune for presenting rather complete calculations on the temperature-dependent properties of Ar, Kr, and Xe (the ideal inert-gas solids, hereafter called IGS) based on model potentials and perturbation theory. (We found quite early in our work that an attempt to apply our ideas to Ne at finite temperatures was not very meaningful because of the very large anharmonic effects involved.) Perturbation theory including the leading correction to the quasiharmonic theory is known to be satisfactory for the ground-state energy<sup>10</sup> and,

\* Present address: Naval Research Laboratory, Washington D. C. 20390.

<sup>1</sup> G. K. Horton and J. W. Leech, in *Proceedings of the Seventh International Conference on Low-Temperature Physics, 1960*, edited by G. M. Graham and A. C. Hollis-Hallett (University of Toronto Press, 1961), p. 697; Proc. Phys. Soc. (London) **82**, 816 (1963). See also J. Grindlay and R. Howard, in *Lattice Dynamics*, edited by R. F. Wallis (Pergamon Press, Inc., N. Y., 1965). Throughout the present paper unless otherwise stated we have used the interatomic potential parameters taken from a review by G. K. Horton, Am. J. Phys. **36**, 93 (1968).

<sup>2</sup> P. Flubacher, A. J. Leadbetter, and J. A. Morrison, in *Proceedings of the Seventh International Conference on Low-Temperature Physics*, edited by G. M. Graham and A. C. Hollis-Hallett (University of Toronto Press, 1961), p. 695; Proc. Phys. Soc. (London) **78**, 1449 (1961); R. H. Beaumont, H. Chihara, and J. A. Morrison, *ibid.* **78**, 1462 (1961).

<sup>3</sup> W. Ludwig, J. Phys. Chem. Solids **4**, 283 (1958); G. Leibfried and W. Ludwig, Solid State Phys. **12**, 276 (1961).

<sup>4</sup> A. A. Maradudin, P. A. Flinn, and R. Coldwell Horsfall, Ann. Phys. (N. Y.) **15**, 337 (1961); **15**, 360 (1961); P. A. Flinn and A. A. Maradudin, *ibid.* **22**, 223 (1963). See also the work of D. C. Wallace, Phys. Rev. **131**, 2046 (1964) and R. A. Cowley, Advan. Phys. **12**, 421 (1963).

<sup>5</sup> T. H. K. Barron and M. L. Klein, in *Proceedings of the Eighth International Conference on Low-Temperature Physics, London, 1962*, edited by R. O. Davies (Butterworths Scientific Publications Ltd., London, 1963), p. 415; Proc. Phys. Soc. (London) **82**, 161 (1963); **85**, 533 (1965).

<sup>6</sup> D. G. Peterson, D. N. Batchelder, and R. O. Simmons, Phys. Rev. **150**, 703 (1966); D. N. Batchelder, D. L. Losee, and R. O. Simmons, *ibid.* **162**, 767 (1967); **173**, 873 (1968); D. L. Losee and R. O. Simmons, *ibid.* **172**, 9 (1968); A. O. Urvas, D. L. Losee, and R. O. Simmons, J. Phys. Chem Solids **28**, 2269 (1967).

<sup>7</sup> L. X. Finegold and N. Philips, University of California Report No. UCRL-18409, 1969 (to be published).

<sup>8</sup> H. Fenichel and B. Serin, Phys. Rev. **142**, 490, (1966).

<sup>9</sup> B. Serin and J. U. Trefny, Bull. Am. Phys. Soc. **13**, 178 (1968). See also J. U. Trefny, Ph.D. thesis, Rutgers University, 1968 (unpublished).

<sup>10</sup> J. L. Feldman and G. K. Horton, Proc. Phys. Soc. (London) **92**, 227 (1967).

*a priori*, seemed applicable to IGS at finite temperature also.

In Sec. 2 we briefly review interatomic potentials for inert-gas crystals. While there seems little doubt that nonpairwise additive forces are present in these solids, their exact nature is still somewhat speculative and controversial. We have chosen, therefore, to use simple effective pair interactions as a starting point for our lattice-dynamical calculations. Although an oversimplification, this approximation is likely to work best for the isotropic thermodynamic quantities considered in this paper. For the most part we have chosen to work with central two-body Mie-Lennard-Jones (*m*-6) potentials, restricted to interact between nearest neighbors (nn) only.

In Sec. 3 we indicate the methods used to obtain our numerical results. In particular, we stress the role played by six sums<sup>10</sup> (specifying the anharmonic Helmholtz free energy) whose temperature and volume dependence yields the anharmonic contributions to the thermodynamic properties that are presented in Sec. 4. We show here that for IGS, perturbation theory does have a useful range of validity. We also apply the lowest-order "self-consistent phonon" approximation to Ar and compare the results with perturbation theory.

Section 5 concludes with some brief comments on possible future work in this field.

## 2. INTERATOMIC POTENTIALS

About nine years ago, when the first quasiharmonic theories were presented,<sup>1</sup> the Mie-Lennard-Jones potentials

$$\phi(r) = \frac{6m\epsilon}{m-6} \left[ \frac{1}{m} \left(\frac{\sigma}{r}\right)^m - \frac{1}{6} \left(\frac{\sigma}{r}\right)^6 \right]$$

with *m*=12 or 13 were used as a starting point. Here, we consider the question of whether it is possible to improve on these potentials today.

There has been significant progress in carrying through Hartree-Fock-type calculations for the electronic ground-state energy of Ne and Ar pairs.<sup>11</sup> Unfortunately, the results are accurate only at small distances (*r* ≤ 2.5 Å) and may not be applicable to the crystal. The effect of short-range many-body interactions have been studied recently, especially by Jansen and his collaborators.<sup>12</sup> However, it is generally believed<sup>13</sup> that these interactions do not play a significant role in the temperature-dependent properties of IGS at least for normal crystal densities.

Substantial progress has been made recently in elucidating true pair potentials for these gases together with corrections from the many-body long-range van der Waals forces. The progress in the former<sup>14</sup> has been

possible in part as a result of accurate information on low-density properties such as the second virial coefficients at low temperatures.<sup>15</sup> In the neighborhood of the minimum of the potential-energy curve, such empirical studies still provide the best source of information about the interatomic forces between these "closed-shell atoms." It is surprising that our detailed knowledge of the two-body interatomic potential in, say, Ar is still confined to the asymptotic limits of small separations (energies of the order several eV) and large separations.<sup>16</sup> The situation may improve when the velocity dependence of the total scattering cross section for Ar-Ar collisions becomes available.<sup>17</sup> For the present, we are forced to give heavy weight to properties like the low-temperature virial coefficient as a means of obtaining information about the bowl of the two-body gas potential.

It has been pointed out by Dymond, Rigby and Smith<sup>18</sup> that the (18-6) potential accounts very well for the second virial coefficient measurements of Ar in the dilute gas. We illustrate this result in Fig. 1 and also show that the Barker-Pompe potential<sup>19</sup> is just as satisfactory. The same is true of the pair potential proposed by Munn and Smith<sup>14</sup> and the Kihara potential with the parameters fitted by Weir, Wynn-Jones, Rowlinson, and Saville.<sup>15</sup> It is, of course, well known that there is no unique way of inverting *B*(*T*) data to obtain a potential. We also include in Fig. 1 the *B*(*T*) calculated for a (12-6) all-neighbor AN potential whose parameters were fitted to solid-state data. The inadequacy of this solid-state potential provides a crude demonstration of the presence of many-body forces in the solid.

In this paper we are focusing on the properties of the IGS, and it is standard practice to assume that for many-body effects only triplet interactions are important. Hence, a triple-dipole dispersion interaction, the so-called Axilrod-Teller term, is added to the true pair potential energy to yield a complete potential energy for the solid.<sup>20</sup> The Axilrod-Teller coefficient is calculated from known oscillator strengths.<sup>21</sup> We have followed this procedure and calculated the Debye temperature  $\Theta_\infty$  (Fig. 2) and the ground-state energy (Fig. 3) for Ar using the Barker-Pompe and (18-6) pair potentials.

F. J. Smith, *ibid.* **43**, 3998 (1966); J. H. Dymond, *Chem. Phys. Letters* **2**, 54 (1968).

<sup>15</sup> R. D. Weir, L. Wynn-Jones, J. S. Rowlinson, and G. Saville, *Trans. Faraday Soc.* **63**, 1320 (1967); M. A. Byne, M. R. Jones, and L. A. K. Staveley, *ibid.* **64**, 1747 (1968).

<sup>16</sup> A. E. Kingston, *Phys. Rev.* **135A**, 1018 (1964); J. A. Barker and P. J. Leonard, *Phys. Letters* **13**, 127 (1964).

<sup>17</sup> See for example B. Baratz, Ph.D. thesis, Princeton University, 1967 (unpublished).

<sup>18</sup> J. H. Dymond, M. Rigby, and E. B. Smith, *Phys. Fluids* **9**, 1222 (1966).

<sup>19</sup> J. A. Barker and A. Pompe, *Australian J. Chem.* **21**, 1683 (1968).

<sup>20</sup> J. C. Rossi and F. Danon, *Discussions Faraday Soc.* **40**, 97 (1965); M. L. Klein and R. J. Munn, *J. Chem. Phys.* **47**, 1035 (1967); G. G. Chell and I. J. Zucker, *Proc. Phys. Soc. (London)* **1C**, 35 (1968); and others.

<sup>21</sup> R. J. Bell and A. E. Kingston, *Proc. Phys. Soc. (London)* **88**, 901 (1966).

<sup>11</sup> T. L. Gilbert and A. C. Wahl, *J. Chem. Phys.* **47**, 3425 (1967).

<sup>12</sup> L. Jansen, *Phys. Rev.* **135A**, 1292 (1964).

<sup>13</sup> C. E. Swenberg, *Phys. Letters* **24A**, 163 (1967).

<sup>14</sup> R. J. Munn, *J. Chem. Phys.* **40**, 1493 (1964); R. J. Munn and

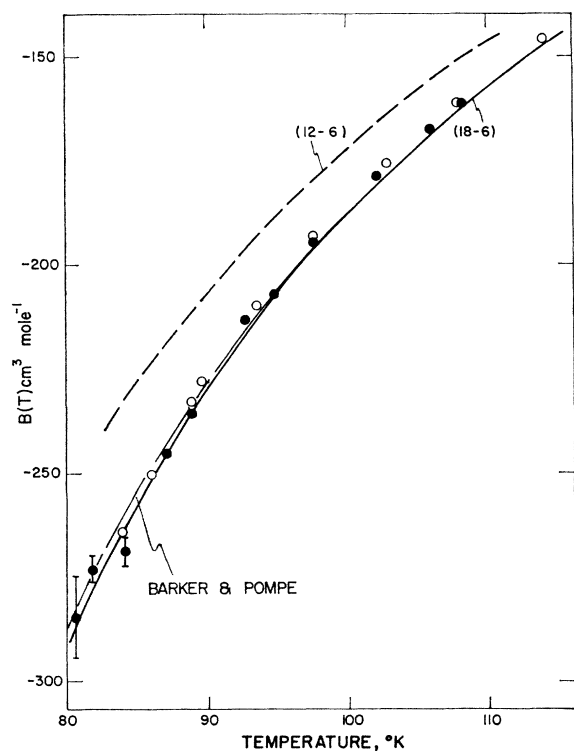


FIG. 1. Second virial coefficient of Ar: The (18-6) potential is from Ref. 18, the Barker-Pompe potential from Ref. 19, and the experimental data from Ref. 15. The (12-6) AN potential parameters were obtained from properties of the solid, Ref. 1.

From Figs. 2 and 3 it is clear that provided the nonadditivity is due to three-body Axilrod-Teller forces, the Barker-Pompe potential is far superior to the (18-6)

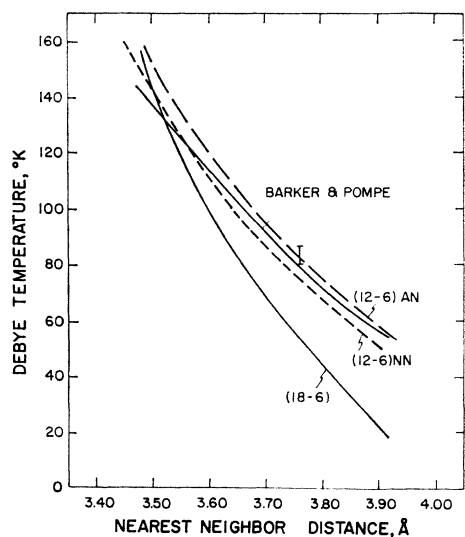


FIG. 2. The high-temperature limit of the Debye temperature  $\Theta_{\infty}^{\circ}$  for Ar as a function of the volume. The error bar indicates the experimental value from Ref. 2. The Barker-Pompe potential is from Ref. 19 and the (18-6) potential from Ref. 18. The (12-6) nn and (12-6) AN potential were taken from Ref. 1.

potential. The latter can then be ruled out as a realistic pair potential on the basis of solid-state data. From the good agreement of the Barker-Pompe potential with these two solid-state properties, it is tempting to imply that nonadditivity, other than three-body Axilrod-Teller forces, gives very small contributions, but we should enter a caveat here. The bulk modulus at 0°K for the Barker-Pompe potential (plus Axilrod-Teller forces) was found to be more than 10% greater than the experimental value. It seems premature therefore to base detailed quantitative studies on the solid on this potential. Moreover, in a recent series of papers, Lucas<sup>22</sup> has considered whether the development of collective dispersion forces in terms of pairs, triplets, etc., is meaningful. It had already been shown earlier by Bade<sup>23</sup> that, particularly for solid Xe, nonadditive interactions involving four atoms are comparable to those involving three atoms. Also, using the (somewhat idealized) Drude oscillator model, Lucas shows that for the heavier solids "the triplet correction to the pair potential cannot be considered as an improvement of the lattice energy with respect to the pair interaction." In fact, he shows that in some cases the perturbation series converges so slowly that the contributions of pair, triplet, etc., must all be summed up for any accurate computations. In his latest paper, Lucas<sup>24</sup> has presented a self-consistent procedure for defining electronic polarization waves in IGS including anharmonic interactions. The method opens the way for including the many-body dipolar

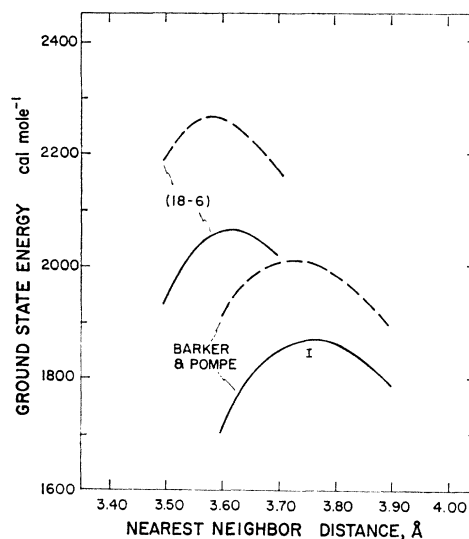


FIG. 3. The Ar ground-state energy as a function of the volume. The experimental result is indicated with error bars on the energy. The long-dashed curve refers to the two-body (gas) potential, while the solid line demonstrates the effect of adding an Axilrod-Teller triple-dipole force.

<sup>22</sup> A. A. Lucas, *Physica* **35**, 353 (1967); *Phys. Letters* **26A**, 640 (1968).

<sup>23</sup> W. L. Bade and J. G. Kirkwood, *J. Chem. Phys.* **27**, 1284 (1957); W. L. Bade, *ibid.* **28**, 282 (1958).

<sup>24</sup> A. A. Lucas, *Phys. Rev. Letters* **21**, A16, 1968.

van der Waals energy of crystals in a more satisfactory fashion. Thus a reliable estimate of the modification of the van der Waals potential term by the dielectric constant of the crystal would be of considerable interest. Until then we must conclude that the correction of the pair potential by an Axilrod-Teller term (Barker-Pompe) in order to obtain a working potential for crystal calculation is incomplete. We are thus forced to work with the old and familiar MLJ (*m*-6) effective potential, and we do so in this paper.

Since our potential is purely *phenomenological*, there is no reason to believe that allowing it to act between all neighbors is, in principle, superior to assuming forces between nearest neighbors only. We shall in most cases therefore concentrate attention primarily on the nn-force model. Results for various other models, including *m*=13, are available from M. L. Klein.

### 3. THEORY

#### Formal Expressions

The thermodynamics used in this paper may be summarized as follows:

$$\begin{aligned} S &= -(\partial F/\partial T)_V, \\ p &= -(\partial F/\partial V)_T, \\ C_V &= -T(\partial^2 F/\partial T^2)_V, \\ B_T &= V(\partial^2 F/\partial V^2)_T = \chi_T^{-1}, \\ C_p - C_V &= \beta^2 TV B_T, \\ \beta/\chi_T &= (\partial p/\partial T)_V, \\ \gamma &= (V/C_V)(\partial S/\partial V)_T, \\ \beta &= (1/V)(\partial V/\partial T)_p. \end{aligned}$$

All quantities involved have their usual meanings. We clearly need

$$F(T, V) = -k_B T \ln Z,$$

with

$$Z = \text{Tr} e^{-\beta H} = \sum_n e^{-\beta E_n}.$$

We write  $H = H_0 + H_2 + H_3 + H_4$ . Then, using perturbation theory, we find

$$F = F_0 + F_2 + F_3 + F_4.$$

Here  $F_0$  is the static lattice energy, and  $F_2$  is the usual quasiharmonic free energy. The detailed expressions can be found in the paper by Feldman and Horton.<sup>10</sup> We will write  $F_3$  and  $F_4$  schematically as

$$F_4 = Z^{-1} \sum_n e^{-\beta E_n} \langle n | H_4 | n \rangle,$$

$$F_3 = -Z^{-1} \sum_{n,m} e^{-\beta E_n} |\langle n | H_3 | m \rangle|^2 / (E_m - E_n).$$

#### Outline of the Calculations

The above expressions were written in a convenient form for numerical calculation by Feldman and Horton. The result was:

$$F_4 = g F_4^R, \quad F_3 = g F_3^R,$$

with

$$F_4^R = (27/4) \{ a_4 I_1(T_R, a_1) + 2a_3 I_2(T_R, a_1) + 4I_3(T_R, a_1) \},$$

$$F_3^R = -\frac{9}{2} \{ a_3^2 S_1(T_R, a_1) + 4a_3 S_2(T_R, a_1) + 4S_3(T_R, a_1) \},$$

$$g = \lambda^2 r^A \phi'' N, \quad a_1 = \phi' / r^2 \phi'',$$

$$a_3 = r^2 \phi''' / \phi'', \quad a_4 = r^A \phi^{IV} / \phi'',$$

$$\lambda = (h/r^3) (M \phi'')^{1/2}, \quad T_R = kT / \lambda r^A \phi'' \approx 2.6T / \Theta_\infty,$$

where  $N$  is the number of atoms,  $\phi^n = (\partial/\partial r)^n \phi$ , and  $M$  is the atomic mass. The details of the evaluation of the  $S_i(T_R, a_1)$  have been published elsewhere,<sup>25</sup> and sample values of the  $I_i(T_R, a_1)$  are given in Table I.

In order to carry out the volume and temperature derivatives listed above, we must obtain a suitable analytical representation for the functions. We used a (6,4) Padé approximant in  $T^2$  to describe their  $T_R$  dependence. In this way we get the correct asymptotic behavior and adequate numerical accuracy. For the  $a_1$  dependence we also used a Padé approximant. We were careful to take into account the volume dependence of *both*  $a_1$  and  $T_R$  when carrying out the various derivatives. As discussed elsewhere,<sup>25</sup> our accuracy is least

TABLE I. Typical values of the sums  $I_i(T_R, a_1)$ .

$a_1$	$10^2 I_1$	$10^2 I_2$	$10^2 I_3$	$T_R$
-0.02	2.765	14.62	12.48	0.00
	2.767	14.64	12.59	0.14
	2.844	15.10	13.02	0.32
	3.017	16.12	14.09	0.44
0.00	4.247	23.17	21.20	0.80
	19.11	107.0	103.8	2.30
	2.582	13.61	11.52	0.00
	2.584	13.62	11.53	0.14
0.02	2.642	13.97	11.91	0.32
	2.781	14.78	12.76	0.44
	3.814	20.65	18.60	0.80
	16.57	92.07	87.72	2.30
0.04	2.425	12.74	10.70	0.00
	2.426	12.75	10.71	0.14
	2.471	13.02	11.00	0.32
	2.584	13.67	11.68	0.44
0.06	3.464	18.64	16.56	0.80
	14.57	80.37	75.42	2.30
	2.287	11.98	10.00	0.00
	2.288	11.99	10.01	0.14
0.08	2.324	12.20	10.24	0.32
	2.417	12.74	10.79	0.44
	3.175	20.65	18.60	0.80
	12.94	70.99	65.75	2.30
0.10	2.166	11.32	9.39	0.00
	2.167	11.32	9.40	0.14
	2.195	11.49	9.58	0.32
	2.273	11.94	10.04	0.44
0.12	2.932	15.63	13.57	0.80
	11.61	63.33	57.96	2.30

<sup>25</sup> M. L. Klein, V. V. Goldman, and G. K. Horton, Proc. Phys. Soc. (London) (to be published).

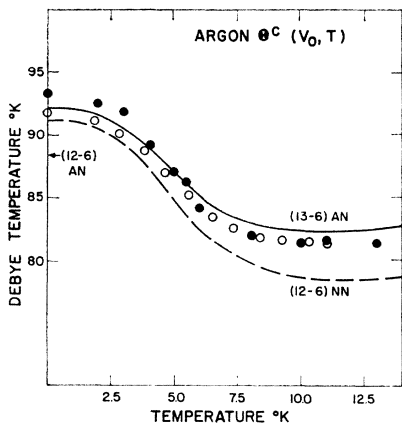


FIG. 4. The low-temperature behavior of the Ar heat capacity at constant  $0^\circ\text{K}$  volume as illustrated by a Debye  $\Theta$  plot; all-neighbor versus nearest-neighbor models. The experimental data are from Ref. 2 (full circles) and Ref. 7 (open circles).

near  $T=0^\circ\text{K}$ . But in this limit, we can use the reliable  $T=0^\circ\text{K}$  results of Barron and Klein<sup>5</sup> and others<sup>26</sup> to guide us.

#### 4. RESULTS

##### Low-Temperature Heat Capacity

We first confine ourselves to a temperature region in which volume expansion and  $C_p-C_v$  corrections can be neglected. In this region the heat capacity is best presented in the form of a  $\Theta$  curve. This is done in Figs. 4-6 for Ar, Kr, and Xe, respectively. The nn results were obtained as described in Sec. 3. The AN curves were obtained by noting that for the temperature range in question, anharmonic contributions to  $C_p$  are essen-

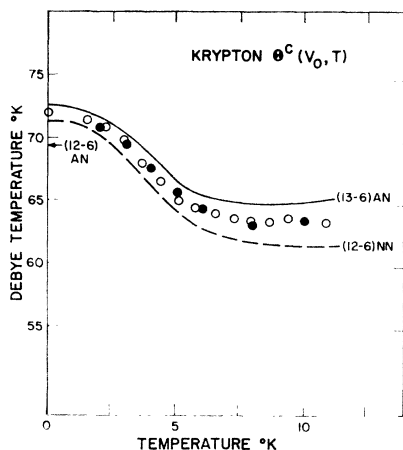


FIG. 5. Low-temperature behavior of the Kr heat capacity at constant  $0^\circ\text{K}$   $M$  volume as illustrated by a Debye  $\Theta$  plot; all-neighbor versus nearest-neighbor models. The experimental data are from Ref. 2 (full circles) and Ref. 7 (open circles).

<sup>26</sup> C. Feldman, Ph.D. thesis, Rutgers University, 1967 (unpublished); J. Brown and G. K. Horton, *Can. J. Phys.* **45**, 2995 (1967).

tially temperature-independent, so that we could simply introduce Barron and Klein's anharmonic  $\Theta_0^c$  into Horton and Leech's quasiharmonic calculation.

The measurements of  $C_p$  are due to Finegold and Philips, to Morrison *et al.*, and to Fenichel and Serin.  $\Theta_0^c$  for Ar and Kr is known to about 0.3%, and for Xe to about 1.4%. In Ar, near  $T=0^\circ\text{K}$ , the  $\Theta^c(T)$  of Morrison *et al.* are about 1.5% too high, a result already surmised by Barron and Klein.  $\Theta^c(T)$  values for Xe are unfortunately less accurate than the Ar and Kr data, especially for  $10 < T < 20^\circ\text{K}$ . Recent measurements by Serin and Trefny<sup>9</sup> suggest that the  $\Theta^c(T)$  for Xe which we have quoted is somewhat low in this temperature range.

Our results show that (13-6) AN potentials give a good over-all account of the low-temperature  $C_p$  of Ar

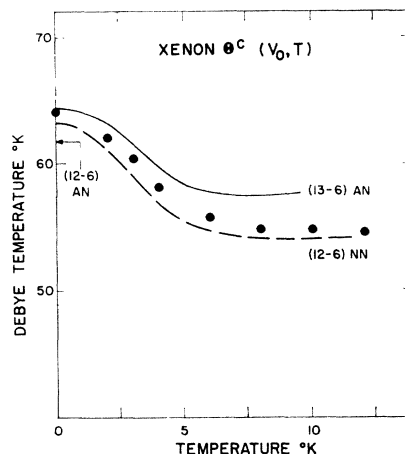


FIG. 6. Low-temperature behavior of the Xe heat capacity at constant  $0^\circ\text{K}$   $M$  volume as illustrated by a Debye  $\Theta$  plot; all-neighbor versus nearest-neighbor models. The experimental data are from Ref. 8.

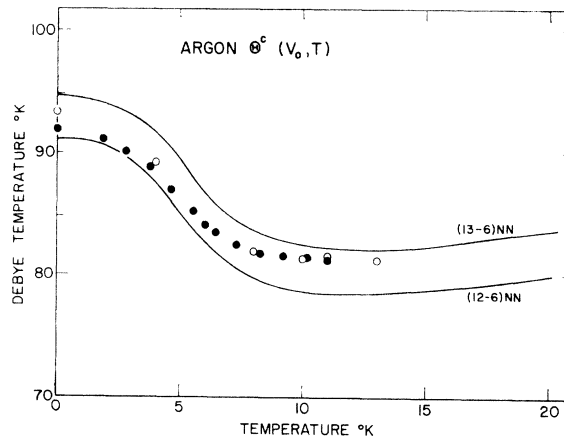


FIG. 7. Low-temperature Debye  $\Theta$  plots for Ar showing the dependence of the theory on the repulsive power in the  $(m-6)$  nn potential. The experimental data are from Ref. 2 (open circles) and Ref. 7 (full circles). The theoretical calculations correspond to the  $0^\circ\text{K}$   $M$  volume.

and Kr. The (12-6) AN model, whose  $\Theta_0^\circ$  is indicated by an arrow on our figures, is not compatible with the experimental data on Ar, Kr, and Xe. This result agrees with the conclusion of Brown and Horton<sup>27</sup> who analyzed the phonon dispersion curves for Kr obtained by Daniels *et al.*<sup>28</sup> The possibility mentioned by Brown and Horton that a (14-6) nn model could describe the properties of solid Kr as a realistic potential can now be safely discarded. It is clear that the (12-6) nn potential gives a fair quantitative description of the low-temperature heat capacity of all three solids. (The excellent agreement for Xe may be due, in part, to experimental difficulties alluded to above.)

In Figs. 7-9 we show the effect of changing  $m$  in the nn potential. Clearly the nn potential is not quite able to account for the fine details of the temperature

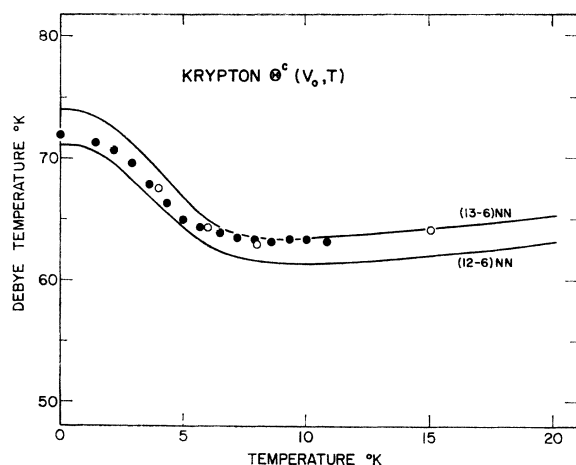


FIG. 8. Low-temperature Debye  $\Theta$  plots for Kr. The legend is the same as that for Fig. 7.

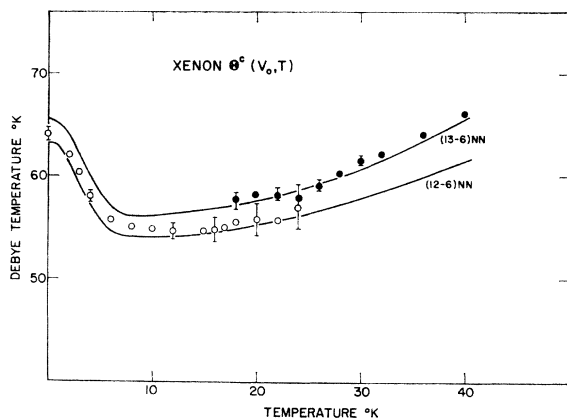


FIG. 9. Low-temperature Debye  $\Theta$  plots for Xe. The legend is the same as for Fig. 7 except that the experimental data are from Refs. 8 and 9.

<sup>27</sup> J. Brown and G. K. Horton, Phys. Rev. Letters **18**, 647 (1967).

<sup>28</sup> W. B. Daniels, G. Shirane, B. C. Fraser, H. Umabayashi, and J. A. Leake, Phys. Rev. Letters **18**, 548 (1967).

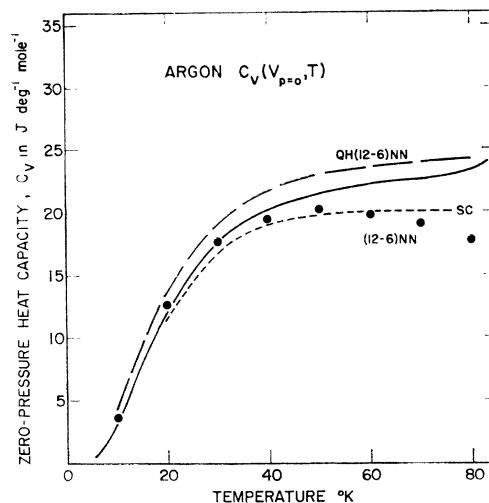


FIG. 10. Heat capacity  $C_V$  of Ar. The circles are the perturbation theory results for the (12-6) nn model. The quasi-harmonic curve QH (12-6) nn is included as a reference point to gauge the magnitude of the explicit anharmonic effects. The sc curve is for a (12-6) nn model calculated in the lowest order self-consistent phonon approximation. The solid unlabeled curve is derived from the experimental data in Ref. 6 and Ref. 2.

dependence of the heat capacity, and hence the true frequency spectrum of these solids. In particular, these models give too large a density of vibrational states at low frequencies.

#### $C_V$ at Constant Pressure (High Temperatures)

The specific heat was evaluated for the calculated equilibrium volume at atmospheric pressure, and the results are shown in Figs. 10-12. The calculated high-temperature deviations from the Dulong and Petit law are very large. Because of this, we must be concerned about the validity of perturbation theory. This point is made clearer by examining the result of including in a self-consistent fashion all even higher derivatives in the potential. For argon  $C_V$  shown in Fig. 10, the appro-

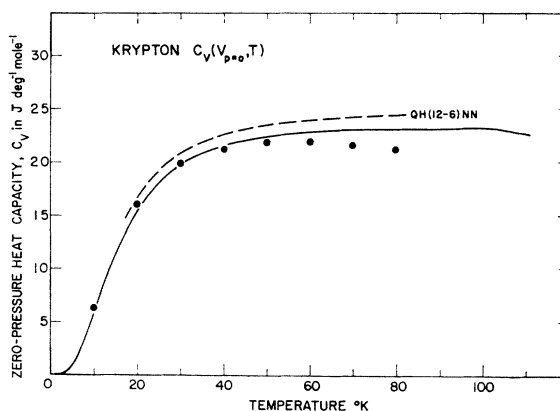


FIG. 11. Heat capacity  $C_V$  of Kr. The legend is as in Fig. 10.

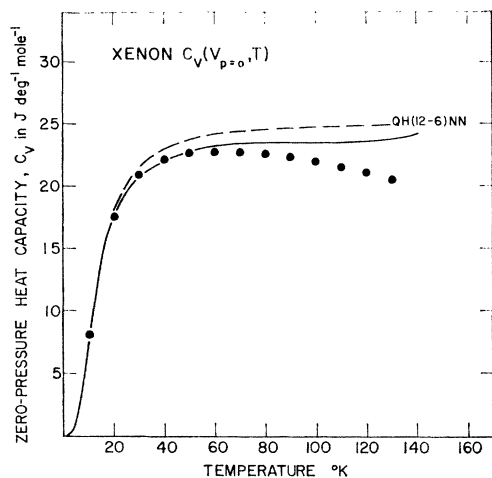


FIG. 12. Heat capacity  $C_V$  of Xe. The legend is as in Fig. 10 except that the experimental data are from Ref. 9.

appropriate curve, labeled self-consistent phonon approximation is for a (12-6) nn potential calculated by the method of Gillis, Werthamer and Koehler.<sup>29</sup> Although it shows a large anharmonic effect, its temperature dependence is in much better accord with experiment than the high-temperature perturbation theory (pt) results. Moreover, as we approach the melting point  $C_V$  for the lowest-order self-consistent scheme (sc) is larger than the pt results. We recall that the sc results themselves are unsatisfactory at all temperatures due to the omission from the calculation of odd derivatives of the potential. How-

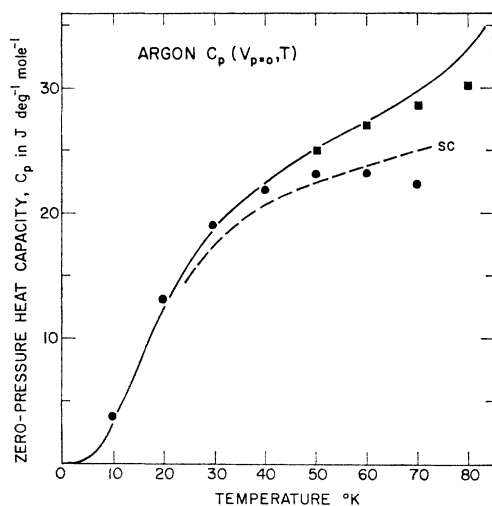


FIG. 13. Heat capacity  $C_p$  of Ar. The circles are perturbation theory results for a (12-6) nn potential. The sc curve is calculated for the same potential in the lowest-order self-consistent phonon approximation. The solid unlabeled curve is derived from the experimental data of Ref. 2. The squares are the quantum-cell-model calculations of Zucker (Ref. 30).

<sup>29</sup> N. Gillis, N. R. Werthamer, and T. R. Koehler, Phys. Rev. **165**, 951 (1968).

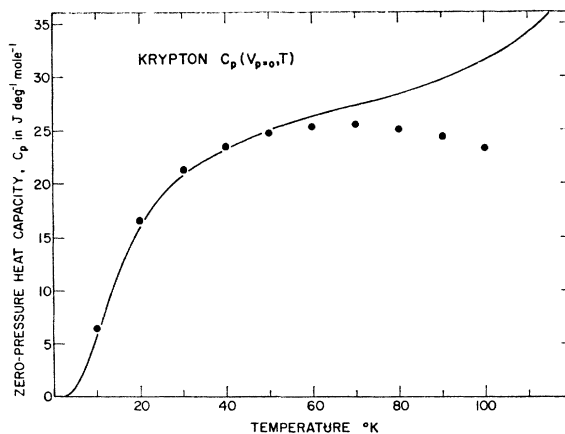


FIG. 14. Heat capacity  $C_p$  of Kr. The circles are the perturbation theory results for a (12-6) nn potential. The solid unlabeled curve is derived from the experimental data of Ref. 2.

ever, precisely because of this they will provide a crude lower bound for the high-temperature  $C_V$ . Hence the pt results are probably spurious at temperatures for which  $C_V(sc) > C_V(pt)$ .

#### $C_p$ at Constant Pressure

What is often measured in the laboratory is  $C_p$  at constant pressure. So we have calculated  $C_p$  for the zero-pressure volume of each temperature. Our results are shown in Figs. 13-15. The unlabeled solid line in each case represents the experimental results. No significant corrections were required in this rather direct confrontation between theory and experiment. We will confine our comments to Ar (Fig. 13), Kr and Xe behave similarly. Below one-third of the melting temperature, perturbation theory is in quite satisfactory agreement with experiment. Above this temperature pt

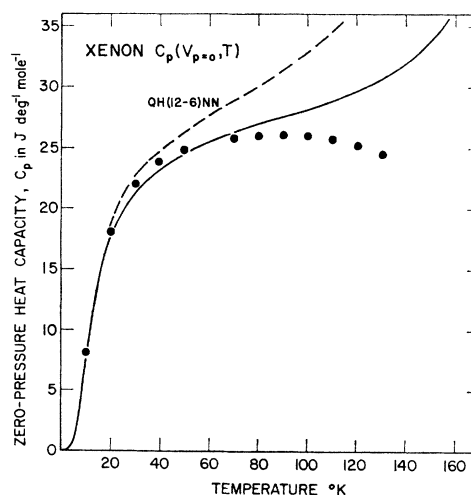


FIG. 15. Heat capacity  $C_p$  of Xe. The legend is the same as that for Fig. 14 except that the data are from Ref. 9.

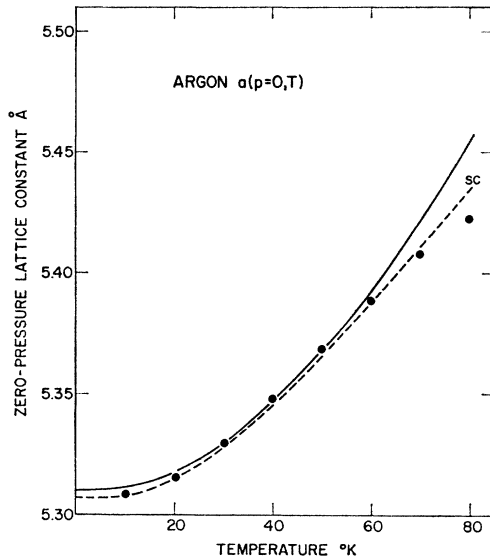


FIG. 16. Lattice constant of Ar. The circles are the perturbation theory results for the (12-6) nn potential. The curve labeled sc is for the same potential calculated in the lowest-order self-consistent phonon approximation. The unlabeled curve is derived from the experimental data of Ref. 6.

results fall below sc. This spurious effect we attribute to a breakdown of pt (to the order considered here). However, since we have not carried through detailed AN calculations we cannot rule out the possibility that our nn potentials are to blame, but this explanation seems unlikely to us. The sc results themselves are not too good either since near the melting point, they predict a  $C_p$  of  $\sim 26 \text{ J deg}^{-1} \text{ mole}^{-1}$  compared to the Dulong

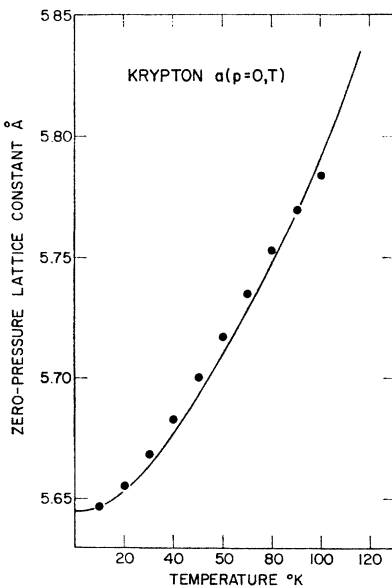


FIG. 17. Lattice constant of Kr. The legend is the same as that for Fig. 16.

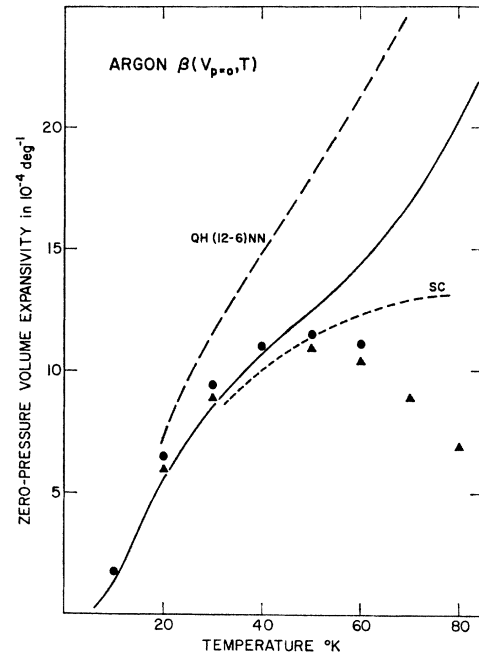


FIG. 18. Expansivity of Ar. The circles and triangles correspond to perturbation theory results for (12-6) nn and (13-6) nn potentials, respectively. The curve labeled sc is for the (12-6) nn potential in the lowest-order self-consistent phonon approximation. The quasi-harmonic curve QH (12-6) nn is included so that the explicit contribution of the anharmonicity can be seen. The unlabeled curve is derived from the experimental results of Ref. 6.

and Petit value of  $25 \text{ J deg}^{-1} \text{ mole}^{-1}$ . The experimental result is  $\sim 35 \text{ J deg}^{-1} \text{ mole}^{-1}$ . It is rather sad that neither theory can challenge the naive quantum-mechanical cell model<sup>30</sup> in the high-temperature region (see Fig. 13).

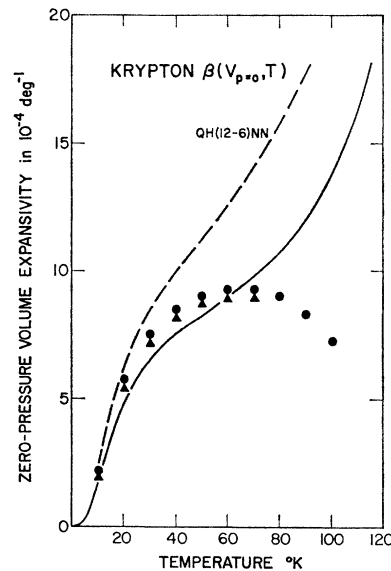


FIG. 19. Expansivity of Kr. Legend is the same as for Fig. 18.

<sup>30</sup> I. J. Zucker, *Phil. Mag.* 3, 987 (1958).



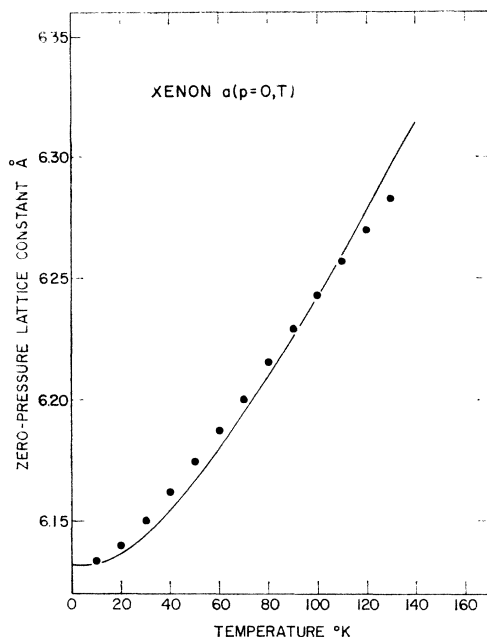


FIG. 20. Lattice Constant of Xe. The circles are perturbation theory results for the (12-6) nn potential. The full curve is derived from the data of Ref. 9.

#### Lattice Constant and Thermal Expansion Coefficient

The lattice constant and the thermal expansion coefficient of solid Ar and Kr have recently been measured with great accuracy by Simmons and his collaborators, and their results are shown in Figs. 16, 17, 18, and 19, respectively, together with our perturbation results. Again, pt gives a fair account of the experimental results below about one third of the melting temperature. However, even in this region 20% discrepan-

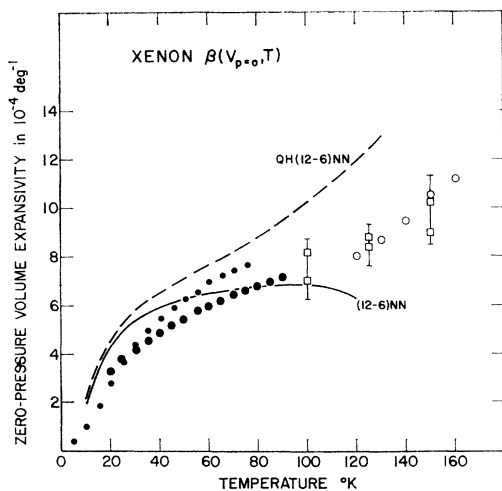


FIG. 21. Expansivity of Xe. The full curve is the perturbation theory result for a (12-6) nn potential. The quasiharmonic curve is included so that the explicit contribution of the anharmonicity can be seen. The data (dots—Sears and Klug; full circles—Manzhelii, Gravlko, and Voitovich; open circles—Gravlko and Manzhelii) are taken from Ref. 31. The squares are taken from Ref. 33.

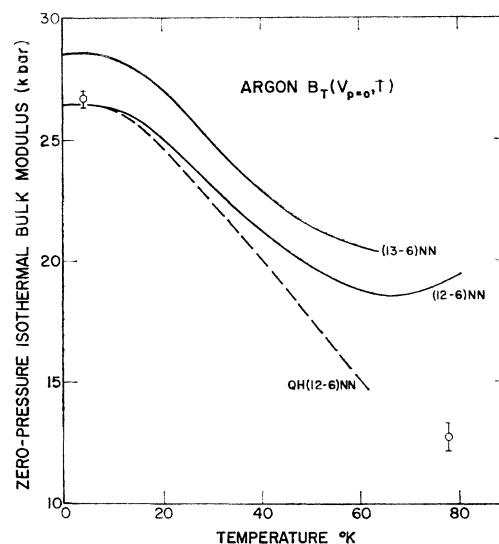


FIG. 22. Isothermal bulk modulus of Ar (zero pressure). The curve labeled (12-6) nn and (13-6) nn are perturbation theory results. The quasiharmonic curve QR (12-6) nn is also shown. The data are from Ref. 6.

cies exist between the models and the experimental expansivities, a situation to which we will return later in connection with the temperature dependence of Grüneisen's  $\gamma$ . At higher temperatures the pt results show the anomalous behavior noted earlier. Anharmonic contributions to  $\beta$  are very large above one-third of the melting temperature and in this region our perturbation theory results cannot be trusted.

For argon, we have also calculated the lowest-order self-consistent phonon (SC) results. It is clear that the lowest-order scheme is incomplete.

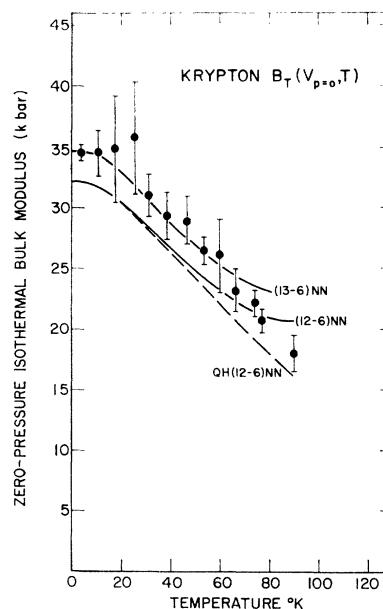


FIG. 23. Isothermal bulk modulus of Kr (zero pressure). Legend is the same as that for Fig. 22.

The experimental data<sup>31</sup> for Xe are not of the same quality as those for Ar and Kr. They are quoted in Figs. 20 and 21 where a comparison with theory is made. In Figs. 18, 19, and 21 we also show the quasiharmonic expansivities. Although they cannot properly predict the correct magnitudes, they do predict the correct general "shape" of the expansivity curves. This suggests that the real crystal behaves like a quasiharmonic solid and that at high temperatures especially, our pt treatment is lacking in some crucial aspect.

### Isothermal Bulk Modulus

Our results are displayed in Figs. 22–24. Again, at high temperatures the pt results show a strange temperature dependence. Up to about one-third of the melting point the pt results with  $m=12$  or 13 give a good account of the experimental data. As with the expansivity, the quasiharmonic approximation shows a more reasonable temperature dependence than pt.

### Grüneisen Parameters at $p=0$ Volumes

In Fig. 25 we show the (12-6) nn results for Ar, Kr, and Xe and compare these with experiment. A number of different measurements contribute to each value of  $\gamma = (V\beta B_T/C_V)$ ,  $C_V = C_p - \beta^2 T B_T V$ . Hence there is some uncertainty in the experimental values we quote. The

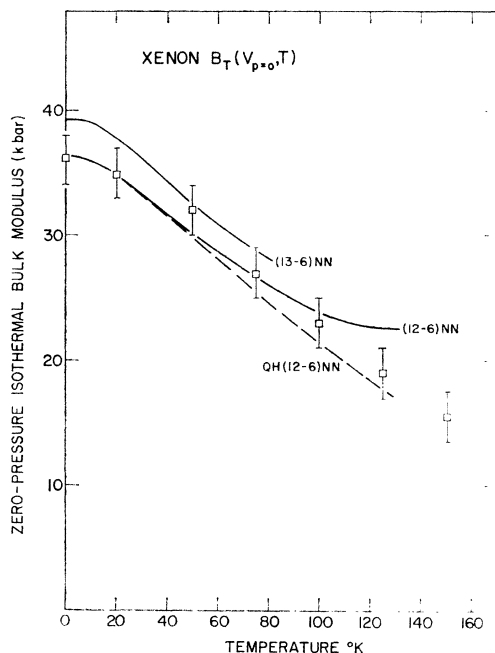


FIG. 24. Isothermal bulk modulus of Xe (zero pressure). Legend is the same as for Fig. 22, except that the data are from Ref. 33.

<sup>31</sup> D. R. Sears and H. P. Klug, *J. Chem. Phys.* **37**, 3002 (1962); V. G. Manzhelii, V. G. Gravilko, and E. I. Voitovich, *Fiz. Tverd. Tela* **9**, 1483 (1967) [English transl.: *Soviet Phys.—Solid State* **9**, 1157 (1967)]; V. G. Gravilko and V. G. Manzhelii, *Fiz. Tverd. Tela* **6**, 2194 (1964) [English transl.: *Soviet Phys.—Solid State* **6**, 1734 (1964)].

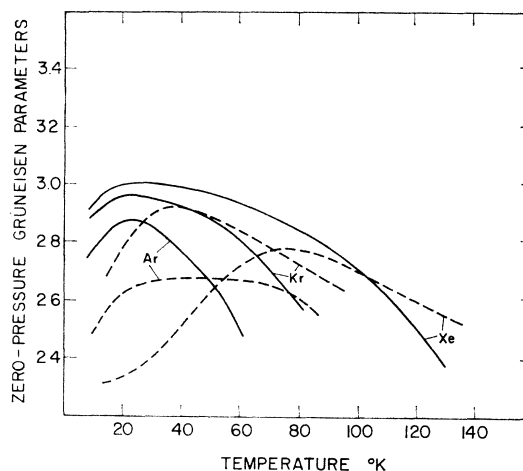


FIG. 25. Grüneisen parameters for Ar, Kr, and Xe (zero pressure). The full curves are calculated for (12-6) nn potential and the dashed curves are experimental curves derived from the data of Refs. 2, 6, 8, 9, 31, and 32.

error bars are difficult to assess and vary with temperature and mass. Above about one-third of the melting temperature, both the experimental results and the theoretical curves show a characteristic fall off. The theoretical  $\gamma$ 's fall much more rapidly than the experimental ones. We attribute this to the breakdown of perturbation theory to which we have drawn attention earlier. At lower temperatures our theoretical results do not decrease with decreasing temperature the way the experimental curves do. Although the latter are most uncertain at low temperatures, there seems to be a real discrepancy here. This we attribute to the inability of our model potentials to account well enough for the expansivity.

### $pT$ Isochores

In Fig. 26 we show two  $pT$  isochores for Ar based upon a (12-6) nn potential. The explicit anharmonic

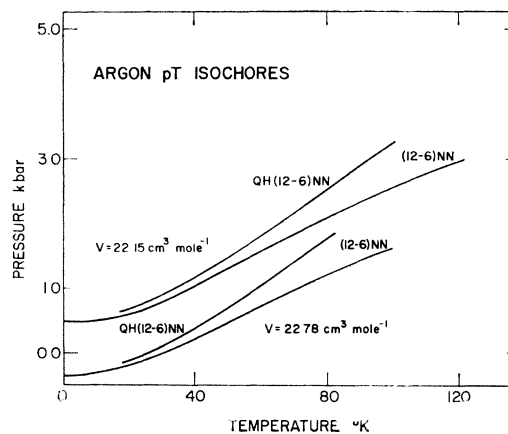


FIG. 26.  $pT$  isochores for Ar. The curves labeled (12-6) nn are the perturbation theory results and the quasiharmonic curves QH (12-6) nn are included so that the explicit anharmonic contribution can be seen.

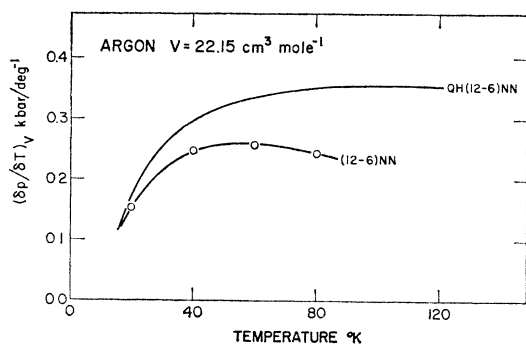


FIG. 27. The temperature dependence of  $(\partial p/\partial T)_V$ . The curve labeled (12-6) nn is the perturbation theory result and the quasi-harmonic curve QH (12-6) nn is included so that the explicit anharmonic contribution can be seen.

contribution to the isochore is large. From the work of Crawford and Daniels<sup>32</sup> we know that the  $V = 22.15\text{-cm}^3\text{-mole}^{-1}$  crystal melts at about  $180^\circ\text{K}$ . At high temperatures our pt results are not to be trusted, so that the inflection in the  $pT$  curve at about one-half the melting point is probably spurious. This point is made clearer by examining  $(\partial p/\partial T)_V$  and this is shown in Fig. 27.

#### $pV$ Isotherms

$pV$  isotherms are shown for Xe in Fig. 28 for three temperatures for an (11-6) nn model. This model fits the data very well especially at high temperatures as already pointed out by Swenson<sup>33</sup> and Zucker.<sup>34</sup> The data points quoted show the typical scattering of the results. The solid lines represent the smoothed experi-

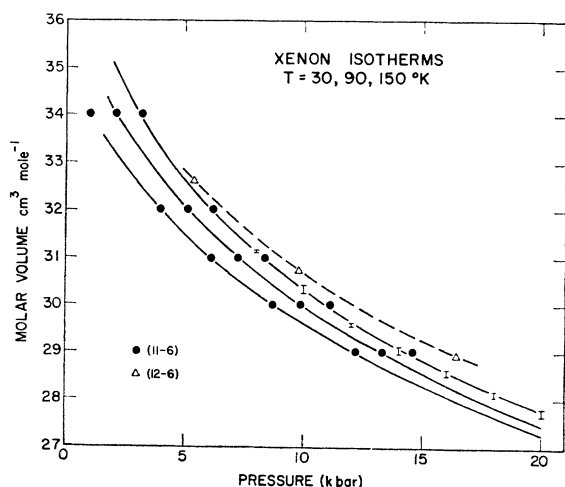


FIG. 28.  $pV$  isotherms for Xe. The full curves are derived from the data of Ref. 33. The full circles are perturbation theory results calculated for an (11-6) nn model. The triangles are results for a (12-6) nn model at  $150^\circ\text{K}$  only.

<sup>32</sup> R. K. Crawford and W. B. Daniels Phys. Rev. Letters **21**, 367 (1968). See also R. K. Crawford, Ph.D. thesis, Princeton University, 1968 (unpublished).

<sup>33</sup> J. R. Packard and C. A. Swenson, J. Phys. Chem. Solids **24**, 1405 (1963).

<sup>34</sup> I. J. Zucker, Nuovo Cimento **54B**, 177 (1968).

mental data and the circles our calculations. Unfortunately there seems to be no systematic pattern emerging from the equation-of-state studies. The (12-6) nn model which does reasonably well for other properties fails completely here.

#### 5. CONCLUSION

In this paper we apply the Born-von Karman theory of lattice dynamics and its generalizations to the ideal inert-gas solids. This theory assumes that the root-mean-square (rms) deviation of the atomic nuclei about their mean positions in a crystal is small compared to the lattice spacing and that the ratio of these two quantities is a meaningful small parameter in a perturbation expansion.

Although to our knowledge the validity of the theory has not been questioned in this situation, we found to our surprise that for the various properties studied in this paper the theory is inapplicable to Ne, and for Ar, Kr, and Xe it is only valid for rms deviations of about 6% or less, i.e., up to about a third of the melting temperature. For  $T \lesssim \frac{1}{3}T_{\text{melting}}$  the over-all features of both the magnitudes and temperature dependences of the thermodynamic properties of solid Ar, Kr, and Xe can be understood on the basis of short-range central interatomic forces. At higher temperatures, serious discrepancies exist between our calculations and experiment; it is shown that these are due to the failure of the conventional truncated perturbation expansion of the partition function rather than to our idealized choice of interatomic potential.

Clearly an improvement over the present investigation would be desirable in two respects. Firstly, a better expansion of the partition function is required for higher temperatures, and there already exists evidence that this can be done.<sup>35</sup> Secondly, refinement in our knowledge of the interatomic forces in the so-called simple solids is needed.

#### ACKNOWLEDGMENTS

We should all like to thank the U. S. Air Force Office of Scientific Research for supporting many phases of this work under Grant No. AFOSR 68-1372. One of us (JLF) would also like to acknowledge the support of the Army Research Office (Durham) and NASA through the RPI Interdisciplinary Materials Research Center. It is a pleasure to thank L. X. Finagold, J. U. Trefny, B. Serin, V. V. Goldman, R. O. Simmons, and their co-workers for letting us see and quote their results freely before publication. At various stages of this work we have also had discussions with T. H. K. Barron, D. A. Benson, R. K. Crawford, W. B. Daniels, P. A. Flinn, T. Keil, T. R. Koehler, A. A. Maradudin, L. H. Nosanow, R. E. Peierls, and N. R. Werthamer.

<sup>35</sup> P. Choquard, in *The Anharmonic Crystal* (W. A. Benjamin, Inc., N. Y., 1967). For a preliminary application of Choquard's method see V. V. Goldman, G. K. Horton, and M. L. Klein, Phys. Rev. Letters **21**, 1527 (1968); Phys. Letters **25A**, 341 (1968).